1 **Title** Studying the spatial structuring of chemical elements through the prism of community and
2 landscape ecology
3
4 **Authors**: Anne McLeod, Shawn Leroux[2], Chelsea L. Little[3], François Massol[4], Eric Vander
5 Wal[2], Yolanda F. Wiersma[2], Isabelle Gounand[5], Nicolas Loeuille[5], Eric Harvey[6]
6
7 1 School of Biological Sciences, University of Canterbury, Christchurch, NZ
8 2 Department of Biology, Memorial University of Newfoundland, St. John's, CA
9 3 School of Environmental Science, Simon Fraser University, Burnaby, B.C. Canada
10 4 Univ. Lille, CNRS, Inserm, CHU Lille, Institut Pasteur de Lille, U1019 - UMR 9017 - CIIL -
11 Center for Infection and Immunity of Lille, F-59000 Lille, France
12 5 Sorbonne Université, Université Paris Cité, Université Paris Est Créteil, CNRS, INRAE, IRD,
13 Institut d'Ecologie et des Sciences de l'Environnement de Paris (UMR7618), 75005 Paris,
14 France
15 6 Centre de Recherche sur les Interactions bassins-Versants – Écosystèmes aquatiques (RIVE),
16 Université du Québec à Trois-Rivières, G9A 5H7, Canada.
17
18 **Corresponding author**. Eric Harvey, Centre de Recherche sur les Interactions bassins-Versants
19 – Écosystèmes aquatiques (RIVE), Université du Québec à Trois-Rivières, G9A 5H7, Canada,
20 eric.harvey@uqtr.ca, tel : 514 977 5180
21
22 **Running Title:** The spatial structuring of chemical elements
23
24 **Keywords:** meta-ecosystem, zoogeochemistry**,** biogeochemistry, distribution models, ecological
25 stoichiometry, beta-diversity, elemental hotspots
26
27 **Article Type:** Perspective
28
29 **No. words in abstract:** 200
30
31 **No. words in main text:** 7230
32
33 **No. words in each text box:** N/A
34
35 **No. of references:** 77
36
37 **No. of figures, tables, and text boxes:** 5 Figures, 1 Table.
38
39
40
41

48   **Statement of Authorship:**

49   EH and SL designed the concept. All authors contributed to refining the framework. AM coded

50   the analysis to produce the results with contributions from EH, FM and NL. AM produced the

51   final figures. EH and AM wrote the first draft of the manuscript with contributions from SL. All

52   authors contributed to further editing of the manuscript. SL, EVW and YFW contributed the data

53   for the proof of concept.

54

55

56 **Abstract**

57   Approximatively 25 chemical elements are essential for the maintenance, growth and

58 reproduction of all living organisms. Hence, the movement, distribution, and relative proportions

59 of those elements on the landscape should influence the structure and functioning of biological

60 communities. Yet our basic understanding for the spatial distribution of elements across

61 landscapes is limited. Here, we propose to apply tools from community and landscape ecology to

62 study spatial patterns in elements. We illustrate this framework using tree leaves elemental

63 composition and demonstrate how spatial grain and spatial dissimilarity of elements interact

64 leading to predictable patterns in elemental distributions at various spatial scales. Meanwhile,

65 further analysis revealed that potassium and calcium are the most important elemental

66 contributors to spatial dissimilarity in leaf elements, raising new questions about their role in, or

67 response to, distributions of biodiversity and ecosystem functions. Our framework provides a

68 way to integrate abiotic and biotic processes, demonstrating how we can use community metrics

69 to investigate variability of individual elements across landscapes. We conclude by

70 hypothesizing that changes in the evenness or beta-diversity of elements should reflect the

71 structure of biotic communities, providing a long-sought mechanistic link between community

72 and ecosystem processes that can be measured directly in the field.

73

3

Introduction

Approximatively 25 chemical elements are essential for the maintenance, growth and
reproduction of all living organisms (Elser *et al.* 1996; Kaspari & Powers 2016). The field of
ecological stoichiometry has made great progress in understanding how some elements (mainly
C, N and P) influence biotic community structure and stability through resource competition and
stoichiometric imbalance (Leroux & Schmitz 2015; Sterner & Elser 2017; Sentis *et al.* 2022).
Most of this research, however, has been conducted at small spatial extents (e.g., lab, mesocosm,
field sites; (Leroux *et al.* 2017). Consequently, our basic expectations for the spatial distribution
of elements and the drivers of those patterns at larger extents are limited to abiotic components
(e.g. bedrock; Kaspari & Powers 2016). To address this gap, researchers in marine (e.g.,
Galbraith & Martiny 2015), freshwater (e.g., Collins *et al.* 2017), and terrestrial (e.g., Leroux *et
al.* 2017) ecosystems are developing spatially explicit tools and methods for predicting spatial
patterns in elements at landscape/seascape extents.

Patterns of elemental abundance in geographic space are the result of the combined feedbacks of
passive abiotic flows and biotic ecosystem components (e.g., animal transport and deposition of
materials). Biotic influences on a landscape are expected to generate a patchy elemental
distribution characterized by areas with elemental hotspots and coldspots (Bernhardt *et al.* 2017;
McInturf *et al.* 2019). For example, McIntyre *et al.* (2008) demonstrated that the spatial
distribution and nutrient excretion of a diverse neotropical fish community can influence the
elemental distribution of N and P availability in streams and that these neotropical fish
communities can influence the distributions of N and P very differently. To scale up the study of
elemental distribution to regional extents, Leroux *et al.* (2017) proposed stoichiometric

97   distribution models (StDMs) – statistical models akin to species distribution models that make

98   spatially explicit predictions of elemental patterns. Stoichiometric distribution models generate

99   spatial maps of elements based on the measured relationship between elements and

100   environmental parameters (e.g., elevation, land cover), thus filling an important gap in measuring

101   elements across a whole landscape. Such elemental maps can then be used readily to study

102   spatial patterns of specific elements (e.g., percent C or N) or their ratios and can be linked to

103   patterns of resource quality (e.g., Heckford *et al.* 2022).

104

105   Building expectations on what spatial patterns in elements should look like, how they relate to

106   landscape features, and how they relate to the other biotic components of ecosystems is not

107   trivial. There is considerable variation in how different plant and animal species respond to and

108   consequently affect their environment – the scale of these effects is species-specific (see review

109   in Doherty & Driscoll 2018) and demonstrate hierarchical patterns within a species (e.g. Mayor

110   *et al.* 2009). For example, small mammals, such as snowshoe hares or meadow voles have a

111   relatively small home range and short daily movements (e.g., Rizzuto *et al.* 2021). Thus, these

112   smaller mammals interact with their environment at smaller scales than larger mammals (e.g.,

113   Leroux *et al.* 2017). The consequences of this smaller environmental footprint mean they may

114   contribute to more localized hotspots of nutrients. Larger mammals, such as moose, use an

115   environment several orders of magnitude larger than hares or voles in boreal forests (e.g.,

116   Balluffi-Fry *et al.* 2020). Through a larger home range and longer daily movements, these larger

117   animals can potentially create larger hotspots of nutrients or more dispersed nutrient hotspots

118   than animals with small home-ranges (e.g., around den sites; Gharajehdaghipour *et al.* 2016).

119   Movement is just one example of how a biotic component of an ecosystem may impact

120   elemental distributions across spatial scales, another example is demographic processes such as

121   the aggregation or over-dispersion of individuals. A tree (e.g., balsam fir) seedling may extract

122   water and limiting nutrients from a small area of soil surrounding its shallow roots whereas an

123   adult tree will extract these resources and affect a much larger area (Olesinski *et al.* 2011).

124   Alternatively, these plants and animals could be homogenizing resource distributions across their

125   home ranges by depleting hotspots that arise from abiotic influences.

126

127   The effects of these biotic ecosystem components on elemental distribution can have a temporal

128   component as well – foraging for resources whether by the root systems of plants or daily

129   movements of animals, are on a shorter temporal scale then dispersal and migration (e.g., Massol

130   *et al.* 2017). In this way a feedback develops both temporally and spatially, further complicating

131   spatial elemental patterns. For example, Pacific salmon spawning creates a pulse of nutrients

132   every fall (hotspot), which is subsequently used by plants and gradually depleted (cold spot) until

133   the next nutrient pulse (Helfield & Naiman 2001). Meanwhile, abiotic features of ecosystems can

134   also lead to patterns that depend on scale. At a broad spatial and temporal extent, weathering of

135   bedrock contributes to the elemental pool, which then get distributed via abiotic and biotic

136   mechanisms. For example, local hotspots of inorganic nitrogen in soils may develop beside

137   streams and rivers where ground and surface water mix, converging chemically distinct flow

138   paths (Edwards 1998). Human activities are significantly modifying both biotic (Díaz *et al.*

139   2019) and abiotic (Pörtner *et al.* 2022) components of ecosystems with potential knock-on

140   effects on the distribution and flux of elements (see Tucker *et al.* (2018) for examples of how

141   human activities have modified the movement of biotic ecosystem components). Consequently,

142   developing tools or methods to measure and quantify how spatial patterns in elements vary

143   across spatial grains is critical to diagnose how ecosystems are being shaped by the current era of

144   rapid change.

145

146   Here, we apply tools from community and landscape ecology to study spatial patterns in

147   elements (Fig. 1). We aim to explore how spatial grain and spatial dissimilarity of elements

148   interact, leading to predictable patterns in elemental distributions at various spatial scales. In

149   particular, because the distribution of elements across the landscape are the result of combined

150   *element-specific* feedbacks of passive abiotic flows and biotic ecosystem components, we

151   demonstrate how dissimilarity metrics offer a unique way to synthesize how multiple elements

152   vary independently across spatial gradients. We illustrate this framework with an empirical proof

153   of concept in the boreal forest. This proof of concept integrates models of the distribution of

154   elements in birch foliage across two landscapes (Leroux *et al.* 2017) with macro-ecological

155   smoothing techniques (Patrick & Yuan 2019) and dissimilarity analyses to investigate the

156   elemental diversity and variation across spatial grains. We first **a)** generate stoichiometric

157   distribution predictions for N, P, Ca, K, and Mg in birch foliage for our two landscapes. We then

158   **b)** use community ecology approaches to explore elemental dissimilarity in elemental content

159   across spatial scales, and **c)** identify potential elemental hotspots/coldspots including **d)** the

160   critical elements contributing to landscape uniqueness, i.e., hotspots or coldspots. Specifically,

161   we would expect dissimilarity to increase and asymptote at a landscape level dissimilarity value

162   as it is broadly driven by geological processes. We would expect hotspots/coldspots to become

163   more homogeneous across the landscape as spatial grain increases and geological processes

164   dominate biotic processes paralleled with a decrease in amount of core area for critical elements

165   contributing to landscape uniqueness.

166

Using community and landscape ecology to study spatial patterns in elements: conceptual

underpinning

We outline our empirical framework and proof of concept in three steps. We begin with a brief

description of our study system and stoichiometric distribution models (*sensu* Leroux *et al.* 2017)

as applied to this system. Next, we outline our application of tools from community ecology to

quantify different components of beta diversity applied to our proof of concept (Anderson *et al.*

2011; Legendre & De Cáceres 2013). Finally, we borrow metrics from landscape ecology (e.g.,

Wang *et al.* 2014) to measure how dissimilarity of elements varies across spatial grains in our

proof of concept.

176

Proof of concept and stoichiometric distribution models

For our proof of concept, we focused on two boreal forest landscapes (i.e., study areas), hereafter

called Plum Point and Old Man's Pond, on the island of Newfoundland, Canada (see

Supplementary Information 1, Fig A1 for map of study area locations). We clipped foliage

samples from the browse height available to boreal forest herbivores (i.e., leaves and small stems

from between 0.3 and 2 m) of 1 to 6 small trees (i.e., < 3 m) within 10 m radius plots across 106

plots at Plum Point between June 30 and July 7, 2015 (see Leroux *et al.* 2017; Balluffi-Fry *et al.*

2020 for more details on field sampling). We used birch trees (*Betula papyrifera*) < 3 m as part

of these data were originally designed to ask questions about moose foraging and moose only

forage on trees < 3 m. We expect these foliage samples to be indicative of bioavailable elements

for herbivores. In particular, white birch is the primary summer forage for moose and snowshoe

hares (Dodds 1960), some of the major herbivores in this system, and thus white birch foliage

189   serves as a proxy for bioavailable elements on the landscape. Focusing on this tree size, also

190   allows us to control for the possibility that trees of different sizes may differ in their elemental

191   composition. Foliage samples were pooled at the plot level and analysed for N, P, Ca, K, Mg (see

192   Leroux *et al.* 2017 for further details on sampling design and Supplementary Information 1 for

193   details on chemical analysis). We focused on these five elements because they are part of the

194   twenty-five elements essential for life and are among the most studied elements in ecological

195   stoichiometry (Jeyasingh *et al.* 2014), are critical for metabolic activity (Kaspari & Powers

196   2016), and frequently reported in studies of the ionome (or the mineral nutrient and trace element

197   composition of organisms; Parent *et al.* 2013). We omit carbon in our analyses because the

198   stoichiometric distribution models for Carbon had a poor fit (see Fig A2 and Table A1(a) for

199   model fit details). We focus only on N, P, Ca, K, and Mg, however, the approach presented here

200   could be applied to a broader suite of elements. Further, while we demonstrate the utility of this

201   approach in a focused proof of concept on the bioavailable elements in foliage samples, a similar

202   approach to the one presented here could be applied to elements in the soil, other important

203   forage, and other animals and would improve insights into the generality of the patterns observed

204   here. The emergence of synthetic databases of the elemental composition of soils and diverse

205   organisms (e.g., https://stoichproject.wordpress.com/stoich/the-stoich-project/about-the-

206   database/)) may facilitate applications of our approach to different case studies.

207

208   Using this white birch foliage chemical composition and methods described in Leroux *et al.*

209   (2017), we fit StDMs to each element from the Plum Point study area. These StDMs are

210   statistical models that describe foliar elemental composition using environmental and biotic

211   covariates aimed at predicting correlations in organismal stoichiometry. We then extrapolate

212   elemental composition across Plum Point and Old Man's Pond landscapes from the correlations

213   in sampled sites of elemental composition with environmental covariates (Leroux *et al.* 2017).

214   Composition of white birch foliar proportions of mass of N, P, K, Ca, and Mg (i.e., elemental

215   composition; %) were the response variables. Predictor variables included three continuous

216   landscape covariates (i.e., normalized aspect or orientation of slope, slope and elevation), and

217   three categorical landscape covariates (i.e., landcover [coniferous, deciduous or mixedwood],

218   stand (canopy) height, and dominant tree species). For more details on StDM model fits, sample

219   design, and chemical analysis see Supplementary Information 1. We retained the full model for

220   each stoichiometric response to predict white birch across the landscape (R^2 for full models were

221   0.31, 0.42, 0.39, 0.13, and 0.27 for N, P, K, Mg, and Ca, respectively; see Table A1 and Fig. A3

222   – A7 in Supplementary Information 1 for specific details on StDM model fits). Using a raster for

223   each discrete covariate, we then developed stoichiometric composition predictions for foliage in

224   each cell. We then transformed the elemental compositions using a chord transformation

225   (Legendre & Gallagher 2001) based on the guidelines by Legendre & De Cáceres (2013) for

226   community composition data, of which our elemental composition data is akin (see Fig. A10 for

227   scaled elemental composition in the two study areas). In particular, this means that we can

228   calculate elemental dissimilarity using the techniques described in Legendre & De Cáceres

229   (2013) without violating any assumption of these approaches.

230   *Elemental dissimilarity across the landscape*

231   An important concept in community ecology is how species diversity is organized across space –

232   a concept for which many metrics have been developed including alpha and beta diversity. By

233   applying species diversity concepts to elemental composition across space, we can determine if

234   elemental composition varies across space in a predictable fashion. Despite many alpha-diversity

10

235 metrics incorporating both species richness and evenness, the constraints on both elemental

236 diversity and evenness mean that alpha-diversity is too coarse a metric to describe elemental

237 distributions appropriately across the landscape. As an explicit metric of variation, however,

238 Bray-Curtis dissimilarity (or variation in elemental composition between cells across the

239 landscape) is sensitive to deviations in evenness. Therefore, we applied dissimilarity metrics to

240 the transformed StDMs to examine stoichiometric variability across landscapes.

241

242 Before computing dissimilarities, we applied a macroecological spatial smoothing approach

243 (MESS), described in Patrick & Yuan (2019). This approach consists of applying a sliding

244 window across a landscape wherein each spatial window resampling and summarizing of local

245 observations occurs. To apply the MESS approach, a spatial grain (s) for the sampling regions is

246 selected, the number of random subsamples (n) of a given sample size (ss) of local cells within

247 that sampling region is specified, along with the minimum number (mn) of local cells in a given

248 sampling region (see Fig. 1). Using the inset in Fig. 1 as an example we would sample 6

249 subsamples (ss) of each window of size s and do this 3 times (n). By resampling the sub-samples

250 in this way we remove the impact of outliers (see Patrick & Yuan 2019). Similar to Patrick &

251 Yuan (2019), we employed a series of analyses to optimize the sample size (ss) and number of

252 random sub-samples (n) required to ensure sufficient sampling is done to determine the value of

253 the dissimilarity metric with appropriate accuracy (essentially where the changepoint in variation

254 around the Bray-Curtis dissimilarity metric occurred was deemed sufficient sampling; see Fig.

255 A8 and A9 in Supplementary Information 2 for results). Our optimal sample size was 11 (mn =

256 1.5×ss as per Patrick & Yuan 2019), a n of 7, and a spatial grain increasing sequentially from a

257 grain size of 500 m to 5000 m in intervals of 200 m.

258   Dissimilarity metrics are then computed for each random subsample of the region, typically

259   averaged within each region. We calculated total community composition variance as proposed

260   by Legendre & De Cáceres (2013) as our dissimilarity metric which returns values between 0

261   (completely similar cells) and 1 (very dissimilar cells). In this way, we would expect Bray-Curtis

262   dissimilarity to be unaffected by grain size if there is no underlying pattern in elemental

263   distributions, increasing if there is an underlying gradient in elemental distributions, and

264   increasing much more rapidly if elements are aggregated in large patches (see Fig. 2a). Finally,

265   we compared the empirical patterns qualitatively to a null model by randomly shuffling

266   longitude and latitude couplets across elemental percentages and then re-running all analyses on

267   the random data set (100 iterations).

268

269   *Identifying hotspots and coldspots of elemental dissimilarity across the landscape*

270   We can extend our proof of concept to characterize cell uniqueness per study area in terms of

271   elemental contributions by applying the approach presented by Legendre & De Cáceres (2013)

272   and extended by Laliberté *et al.* (2020) (termed local contributions to beta diversity; LCBD).

273   This approach uses sum of squared deviations to characterize individual cells' contributions to

274   elemental beta diversity:

275
$$LCBD = \frac{\sum_{j=1}^{p} s_{ij}}{SS_{Total}} \qquad (1)$$

276   where

277
$$s_{ij} = \left(y_{ij} - \bar{y}_j\right)^2 \qquad (2)$$

278   and

279
$$SS_{Total} = \sum_{i=1}^{n} \sum_{j=1}^{p} s_{ij} \qquad (3)$$

280   Where i is cell and j is element, and y is elemental percentage. As such, this metric identifies the

281   cells that contribute more or less than the mean to beta diversity, acting as a comparative

282   indicator of cell uniqueness with larger LCBD values indicating cells that are more different in

283   terms of elemental composition. Importantly, this metric has been used to identify hotspots, or

284   cells which have unusually rich species compositions, and coldspots, or cells which are species

285   poor, but does not distinguish between the two (Legendre & De Cáceres 2013; Poisot *et al.* 2017;

286   Laliberté *et al.* 2020). We apply this approach to elements to identify unique cells on the

287   landscape – or cells that have unusually high elemental evenness and cells which have unusually

288   low elemental evenness.

289

290   *Identifying critical elements contributing to landscape uniqueness*

291   By applying the framework presented in Legendre & De Cáceres (2013) we can tease out site

292   uniqueness across the landscape, and can determine the individual contributions of each element

293   to each site across the landscape. In particular, we can identify patches where a specific element

294   is the most important contributor to elemental diversity (i.e., elemental contributions to beta

295   diversity; ECBD), and explore how the size of these patches change with grain size. For

296   example, if small foraging movements dominate the transport of elements around the landscape

297   at small grain sizes, we may expect a random configuration of very small patches for each

298   element, while if geochemical processes dominate the distribution of elements at larger grain

299   sizes then we may expect much larger patches for each element.

300

301   Similar to LCBD, our novel application we term, ECBD, uses a sum of squared deviations

302   approach:

$$ECBD = \frac{\sum_{i=1}^{n} s_{ij}}{SS_{Total}} \qquad (4)$$

303

304   Where s_{ij} and SS_{total} are defined as above. To determine patchiness of elemental contributions, we

305   then applied landscape pattern metrics to determine how patches of elemental contributions vary

306   with grain size, and compared these values to the null model randomizations generated earlier in

307   the analysis.

308

309   We applied three spatial pattern metrics – mean core area, perimeter area fractal dimension, and

310   normalized landscape shape index – at the landscape level (see Fig. 2b for examples). These

311   metrics were identified by Wang *et al.* (2014) as suitable metrics to differentiate spatial

312   aggregations of landscapes.

313

314   Mean core area index is defined as the mean of the core areas of all patches belonging to each

315   landscape class (i.e. N, P, K, Ca, and Mg) where core area is defined as all cells that have no

316   neighbours (queen's case) with a landscape class different from their own. If geochemical

317   processes dominated the distribution patterns of elements at larger spatial grains, we would

318   expect the mean core area to increase with spatial grain whereas if mean core decreases with

319   spatial grain biotic ecosystem components (e.g., foraging) may be the drivers.

320

321   The perimeter area fractal dimension is a shape metric describing patch complexity, but is scale

322   independent, and has values between 1 and 2, with values closer to 1 denoting simple shapes and

323   values closer to 2 denoting irregular shapes. If biotic drivers (e.g., foraging movements) were

324   dominating the distribution pattern of elements at finer spatial grains, we may expect shapes with

325 higher overall irregularity (i.e., values closer to 2). However, abiotic drivers such as mixing of

326 surface and groundwater beside streams could also create higher overall irregularity.

327

328 The normalized landscape shape index is also an aggregation metric and describes the ratio of

329 the actual edge length of a landscape class to the hypothetical range of possible edge lengths for

330 this landscape class, although note that this landscape index was one of the metrics shown by

331 Frazier (2022) to be sensitive to variation in scope. This metric ranges from 0 if only one square

332 patch is present to 1 for a maximally disaggregated (i.e., checkerboard) landscape. If

333 geochemical processes were the only processes driving elemental distributions and they only

334 operated at larger spatial grains, then we would expect the normalized landscape shape index to

335 decrease from a value close to one to a value close to zero as spatial grain increases (Fig. 2b).

336 Meanwhile, if biotic ecosystem components such as demographic processes (e.g., aggregation

337 and over-dispersion) were the only processes driving elemental distributions we may expect the

338 normalized landscape shape index to increase from a value close to zero (clumping of species at

339 small grain sizes) to a value close to one at large grain sizes.

340

341 Finally, for these analyses, the pixel size is 6207.943 m^2 and the ratio of extent to grain (i.e.,

342 scope sensu Frazier 2022) is 187,154 and 205,842 for Plum Point and Old Man's Pond

343 respectively.

344

345

346 **A Community Ecology of Elements in Practice: Proof of concept results and discussion**

347 *Proof of concept and stoichiometric distribution models*

348   The white birch foliage StDMs explained between 13 and 42% of variation in the elemental

349   responses for N, P, K, Mg, and Ca (see Table A1 and Fig. A2 – A6 in Supplementary

350   Information 1 for specific details on StDM model fits). The estimated percent nitrogen ranged

351   from 1.90 to 3.67%, the percent phosphorus ranged from 0.16 to 0.42%, the percent potassium

352   ranged from 0.24 to 1.61%, the percent calcium ranged from 0 to 0.62%, and the percent

353   magnesium ranged from 0.03 to 0.24% for Plum Point. At Old Man's Pond the estimated

354   percentages were a little bit higher for all elements except phosphorous. Nitrogen ranged from

355   1.78 to 3.72%, the percent phosphorus ranged from 0.13 to 0.43%, the percent potassium ranged

356   from 0.33 to 1.70%, the percent calcium ranged from 0.10 to 0.70%, and the percent magnesium

357   ranged from 0.11 to 0.24% (see Supplementary Information 3 Fig. A9 for scaled elemental

358   abundances in both study areas). These values are similar to patterns reported for other study

359   areas on the island of Newfoundland (Heckford *et al.* 2022).

360

361   *Elemental dissimilarity indices across the landscape*

362   In our proof of concept, we found that elemental dissimilarity increased with grain size,

363   eventually reaching an asymptotic "landscape level dissimilarity" when the grain size kept

364   increasing. The asymptote is the mean of the null model for our two study areas (Fig. 3). The

365   observed increase in dissimilarity with spatial grain mimics relationships already observed for

366   other components of biodiversity estimates. For example, species richness typically increases

367   rapidly at local scales due to a) stochastic variation in species occupancy patterns among cells

368   with more distant patches expected to demonstrate more differences in species composition (e.g.

369   gradient landscape of Fig. 2a); or b) increasing likelihood of sampling novel habitats as spatial

370   grain increases (e.g., Whittaker 1972; Harrison *et al.* 1992; Koleff & Gaston 2002). A variety of

371   different environmental and organismal factors are hypothesized to drive species dissimilarity at

372   various spatial scales ranging from habitat composition and structure at local scales to topology

373   and dispersal limitation at regional scales (see Table 1 in Barton *et al.* 2013 for more details).

374   Due to the way we carried out our analysis, it is unlikely that we are increasing the likelihood of

375   sampling novel elements as spatial grain increases since all elements were found at every site.

376   Rather, one explanation for what we are observing is a predictable gradient of variation in

377   elemental composition with more distant patches being more dissimilar: as the spatial grain of

378   the analysis increases, we observe an increase in dissimilarity as more dissimilar patches are

379   sampled (e.g., gradient in Fig. 2a vs. large checkerboard).

380

381   The trend we observe here between elemental dissimilarity and grain size suggests a similar

382   change in environmental and organismal drivers with scale. For example, organism movement

383   capacity affects species dissimilarity with species moving to track environmental gradients at

384   fine spatial scales (Kaspari *et al.* 2010). Thus, the rapid increase in elemental dissimilarity with

385   grain size could be related to consumer species distribution and activity including demographic

386   effects, abundance, and consumer movements as they distribute elements across the landscape.

387   Thus, the plateau at the asymptotic "landscape level dissimilarity" (Fig. 3) could be related to

388   differences between large patches driven by landscape features such as aquatic-terrestrial

389   boundaries, i.e., forest patch along the narrow lake on the southwest side of Old Man's Pond (e.g.

390   McClain *et al.* 2003). Our example is only one testable hypothesis. Alternate hypotheses could

391   include variation in light availability, moisture, and plant competitors all of which could alter

392   local elemental composition potentially causing a similar increase in dissimilarity at finer grain

393   sizes.

394

395   Importantly, the dissimilarity in elements across the landscape can be a cause or a consequence

396   of biodiversity, but in either case, theory on nutrient co-limitations and stoichiometry would

397   suggest that greater elemental spatial turnover is indicative of greater biodiversity (Elser *et al.*

398   1996; Chase & Leibold 2009; Harpole *et al.* 2011). For example, if elemental dissimilarity is

399   very low with all elements equally abundant across the landscape, this should lead to biotic

400   homogenization and the dominance by a few species (ones with lower R*, or equilibrium

401   resource level, for the specific homogenous condition). While our study presents some first steps

402   in tackling this question, further studies with species diversity data are needed to tease out these

403   directional relationships. However, recent work suggests that high imbalance in stoichiometric

404   ratios among connected patches (thus higher spatial turnover in elements) can lead to higher

405   productivity at the meta-ecosystem scale because of spatial complementarity in limiting nutrients

406   (Pichon *et al.* 2023).

407

408   *Identifying hotspots and coldspots of elemental dissimilarity across the landscape*

409   In our proof of concept, we demonstrate that at finer grains, the cells with higher local

410   contributions to landscape dissimilarity (i.e., those that more unique than the average site) cluster

411   together at both Plum Point and Old Man's Pond as evidenced by the yellow patches present at

412   grain size 500 m (Fig. 4). A grain size of 500 m corresponds to the scales at which organisms

413   feeding on birch leaves are most active in their foraging – for example snowshoe hares have a

414   home range of 0.027 - 0.042 km^2 (Rizzuto *et al.* 2021) while moose have been shown to have

415   daily movements between 0.5 km and 1.1 km depending on the season (Hundertmark 1998).

416   Whether these patches of high contributions of dissimilarity are a consequence of biotic

417   processes (e.g., foraging movements) or a cause of these biotic processes is unclear, and likely

418   are the result of a complex feedback between abiotic and biotic processes. Large-bodied

419   organisms can move an impressive amount of nutrients within and across ecosystems (Schmitz *et*

420   *al.* 2018), which can lead to the expected succession of hotspots and coldspots in the landscape

421   through source-sink dynamics (sensu Loreau *et al.* 2013 for the extension of the source-sink

422   concept to abiotic fluxes; McIntyre *et al.* 2008; McInturf *et al.* 2019). The clustering of cells with

423   high local contributions to landscape dissimilarity at finer grain sizes could be indicative of these

424   source-sink dynamics. Thus, the chain of cause and consequence generating the observed spatial

425   variation in resource elements is being reconsidered in an exciting junction between

426   biogeochemistry, ecosystem and community ecology.

427

428   As the grain size increases, however, the landscape becomes more homogenous with a greater

429   number of cells exhibiting an intermediate level of uniqueness, and those cells that are most

430   different are more diffuse across the landscape (Fig. 4). Only two larger patches of more unique

431   cells are observed at a grain size of 5000 m for Plum Point. Meanwhile the more unique cells in

432   both Plum Point and Old Man's Pond seem to be concentrated around bodies of water at a grain

433   size of 5000 m. One possible explanation for this is a shift in the driver of these

434   hotpots/coldspots from biotic to abiotic drivers, such as landscape features, for example aquatic-

435   terrestrial boundaries. Likely, it represents a complex feedback between abiotic drivers, such as

436   the mixing of surface and ground waters at the aquatic-terrestrial boundary converging

437   chemically distinct flow paths (Edwards 1998), and biotic drivers, such as terrestrial ungulates

438   foraging on aquatic plants (e.g. moose-aquatic plants relationship; Bump *et al.* 2017). Future

439   work can apply our method to more completely account for the stocks and flows of elements

440 across scales including measuring the elemental footprints (or combination of nutrient stocks and

441 effects of organisms on stocks) of soils, plants and small and large herbivores.

442

443 *Identifying critical elements contributing to landscape uniqueness*

444 In our proof of concept, we observed that in both Plum Point and Old Man's Pond, potassium (K)

445 and calcium (Ca) are the most important contributors to dissimilarity. This is intriguing as many

446 studies to date have been focused on the contributions of the three more abundant elements –

447 Carbon, Nitrogen, and Phosphorus to biotic community structure and stability (e.g., Leroux &

448 Schmitz 2015; Sterner & Elser 2017; Sentis *et al.* 2022). Rather what this result suggests is that

449 the distribution of these less abundant, but essential, elements may be just as important for

450 community structure. Specifically, in both study areas K is more often the most important

451 contributor (see Supplementary Information 3 Fig. A11; Fig. 5). In Plum Point, however, Ca

452 becomes increasingly important as grain size increases, while K becomes less important. The

453 converse occurs in Old Man's Pond where K becomes increasingly more important, but appears

454 to level off at 4000 m. Interestingly, Ca and K are inherently connected in plant nutrition

455 whereby as Ca concentrations decrease, K concentrations increases due to luxury consumption of

456 K and K antagonism whereby K occupies the majority of exchangeable ionic sites (Wilkinson *et*

457 *al.* 2000). Moreover, it has been shown that Ca is generally taken up in amounts corresponding

458 to availability rather than plant requirements (Knecht & Göransson 2004), perhaps explaining the

459 different patterns in the two study areas. Our results highlight the importance of rarely measured

460 elements such as K and Ca for structuring spatial dissimilarity in elements across spatial grains, a

461 result that underscores the difficulties in multi-dimensional ratios given the controversy in ratio

462 approaches for more elements than just N, P, and C (Parent *et al.* 2013).

463

464   There is a decline in mean core area with grain size for both elements in both study areas. The

465   decline is especially pronounced for K in Plum Point (Fig. 5). The decline demonstrates that the

466   landscape gets more homogeneous as grain size increases and occurs most precipitously for Ca

467   in both Plum Point and Old Man's Pond and then levels out at a grain size of 1500 m for both

468   study areas. These declining trends are reflected in the normalized shape index plots where both

469   elements become less aggregated as grain size increases. However, in the Plum Point study area

470   there is a peak for both K and Ca at a grain size of 2000 m, after which the normalized landscape

471   shape index declines. Elements at Plum Point are therefore least aggregated at grain size of 2000

472   m, and the landscape becomes more like a single square patch as grain size increases. At Old

473   Man's Pond the normalized shape index reaches an asymptote for both K and Ca at a grain size

474   of ~3000 m. Examining the perimeter area fractal dimension illustrates that, the shapes of

475   elemental patches across the study area become more irregular as grain size increases, contrary

476   to our earlier speculations. One explanation for this could be the increasing importance of abiotic

477   drivers such as confluence of ground and surface waters at aquatic boundaries at larger grain

478   sizes. Grain size contributes to increasing perimeter area fractal dimension irregularity in both

479   study areas, but does appear to asymptote at a grain size of approximately 2000 m for Ca in both

480   study areas. However, it should be noted that the two study areas have a different scope (ratio of

481   range to extent) and Frazier (2022) showed that some metrics, including the landscape shape

482   index, which we used here, is highly sensitive to variation in scope. Thus, comparisons between

483   the two study areas may be artifacts of differences in scope.

484

485   Much research has determined that elements cluster in two distinct groups based on the

486   competing needs to grow and maintain existing structure (Ågren & Weih 2012; Zhang *et al.*

487   2012). The first reflects plant growth rate and correlates with nitrogen and phosphorus

488   concentrations – elements critical for the metabolism of nucleic acids and proteins (Ågren &

489   Weih 2012). The second reflects maintaining plant structural components requires K, Ca, and

490   Mg, that are critical for cell walls and might be more important for long-lived slow-growing

491   plants (Nakajima *et al.* 1981; Maathuis 2009). The structural elements appeared to be the most

492   important drivers of elemental dissimilarity in white birch tissue across the landscape in our

493   proof of concept. The ECBD metric does not tell us whether elemental importance is caused by

494   low amounts or high amounts of these structural elements, however evidence suggests that K is

495   rarely limiting and excess K availability can contribute to higher growth rates in plants (Maathuis

496   2009). Similarly, Ca is usually abundant in the lithosphere, however, Ca concentrations in plants

497   can fall below a critical threshold in fast-growing tissues which can lead to diseases such as

498   blossom end rot in tomatoes (Maathuis 2009).

499

500   Notwithstanding current challenges in identifying the processes behind elemental importance,

501   the fact remains that we can observe patterns in elemental importance. In meadow systems,

502   studies have shown that in the absence of grazing by sheep, plants become more nutritious with

503   greater concentrations of micronutrients such as Ca (Marrs *et al.* 2020). In the boreal forest,

504   moose are selective herbivores and could be selectively removing nutritious plants that relatively

505   high in N and P in a similar fashion creating elemental coldspots (Pastor *et al.* 1998). Indeed, the

506   observed patterns in elemental importance should have a predictive influence over biodiversity

507   simply because these patterns control the amount of co-limiting nutrients and their spatial

508   turnover (Marleau *et al.* 2015). More specifically, the spatial heterogeneity in resource elements

509   should relate to coexistence dynamics and community structure directly influencing the number

510   of available niches. For example, studies have shown a correlation between plots containing tree

511   species with calcium-rich detritus and a greater diversity and biomass of earthworms (Reich *et*

512   *al.* 2005).

513

514   **Perspectives**

515   Our understanding of how and why chemical elemental concentrations change in space or across

516   scales is currently very poor (Kaspari & Powers 2016), contributing to poor integration of

517   empirical and theoretical metaecosystem research. The spatial distribution of resource elements,

518   however, reflects element-specific feedbacks of passive abiotic and biotic processes, thus

519   dissimilarity in resource elements may contain much of the information necessary to infer key

520   characteristics of biotic communities, and the expected relationship between those characteristics

521   and ecosystem function (Wu *et al.* 2015). Therefore, identifying spatial patterns in resource

522   elements in the landscape may allow regional scale prediction of community structure,

523   biodiversity, and ecosystem function. Moreover, the analysis of spatial patterns in the

524   fundamental building blocks of all life – elements – can pave the way for greater integration of

525   empirical and theoretical metaecosystem research. Such an integration would open significant

526   new opportunities to finally develop a unified field of spatial ecology, from community to

527   ecosystem and landscape level processes. Disentangling the drivers of these patterns is

528   challenging, especially as the direction of causality is not always intuitive and often involves

529   feedbacks between abiotic and biotic ecosystem components (see Ellis-Soto *et al.* 2021 for a

530   guide to measuring the biotic component of spatial ecosystem subsidies). Here, we have

531   presented a framework to explore spatial patterns in elemental distributions from foliage

532   samples; however, the approach we present is timely as it corresponds with a time of recent

533   growth in data on elemental composition of soil and diverse organisms across many different

534   biomes. In this way, we provide ecologists with an additional and critical tool for describing

535   ecosystems (see Table 1 for explicit predictions).

536

537   Dissimilarity of resource elements may be the result of or may affect food web structure. For

538   instance, we know that elemental hotspots tend to appear at locations in the landscape rich in

539   energy and material exchange (e.g., deep-sea hydrothermal vents), or where different chemical

540   reactants are expected to meet (e.g., ecotone between terrestrial and aquatic ecosystems -

541   McClain *et al.* 2003; Bernhardt *et al.* 2017). Different lines of evidence also suggest that

542   organism movement can track those hotspots in the landscape (McNaughton *et al.* 1988;

543   Leimgruber *et al.* 2001; Leroux *et al.* 2017; Balluffi-Fry *et al.* 2020; Kaspari 2020). Recent

544   conceptual and theoretical developments related to metaecosystem theory now challenge our

545   current understanding by suggesting that organisms themselves, through their movement in the

546   landscape and feeding interactions, could generate the emergence of those observed elemental

547   hotspots in the landscape (i.e., zoogeochemistry; Leroux *et al.* 2017; Gounand *et al.* 2018;

548   Schmitz *et al.* 2018; McInturf *et al.* 2019) and potentially diffuse the elemental hotspots

549   generated by abiotic processes. The elemental dissimilarity approach presented here provides a

550   way of measuring some of these elemental patterns across the landscape with the ECBD metric

551   being particularly useful in teasing out the scale at which each element is most important for

552   dissimilarity (see Table 1 for testable hypotheses).

553

554 More than that however, previous research has demonstrated how energy and nutrients in food

555 webs generally come from different trophic pathways that vary in their resource quality and the

556 speed at which energy and materials flow (Rooney *et al.* 2006). Traditionally, stoichiometric

557 analyses focus on ratios, which have proven useful to understand trophic interactions (e.g., Hall

558 2009; Leroux & Schmitz 2015) and co-limitation in competitive communities (e.g., Harpole *et*

559 *al.* 2011; Marleau *et al.* 2015). In particular, these stoichiometric analyses that have focused on

560 the C:N and C:P ratios of resources are a useful way to characterize these different trophic

561 pathways as ecosystems with resources with high (low) C:N ratios tend to be less (more)

562 palatable for herbivores and this decreases (increases) the rate of materials flowing in this

563 pathway (Hall *et al.* 2004; Shurin *et al.* 2006). Our work, however, has demonstrated the role

564 that some of the other less abundant essential elements (e.g. K and Ca) play in landscape

565 elemental dissimilarity – potentially offering additional currencies to tease out some of these

566 relationships. For example, whereas some top consumers focus on one energetic or material

567 pathway, many consumers couple multiple pathways (Rooney *et al.* 2008; Ward *et al.* 2015).

568 Indeed, this coupling of different energetic pathways is an important contributor to ecosystem

569 stability (McCann *et al.* 1998; Rooney *et al.* 2006). We hypothesize that, irrespective of the

570 direction of causality, changes in the evenness or dissimilarity of element ratios should be

571 reflected directly into the structure of biotic communities, providing a long-sought mechanistic

572 link between community and ecosystem processes that can be measured directly in the field.

573 Thus, a community perspective on elemental resources holds promise to synthetize our

574 understanding of biodiversity and ecosystem function across level of organization.

575

576   From an applied perspective, the majority of conservation planning focuses on the protection and

577   restoration of species, populations or communities, despite a call towards "ecosystem-based

578   management" in terrestrial, freshwater, and marine realms. We surmise that, in some cases,

579   elemental hotspots may be important features to protect or restore. For example, natural sodium

580   licks are critical sources of this limiting nutrient for many large ungulate communities in

581   temperate and boreal forest ecosystems (Kaspari 2020). In many ways, a pivot towards

582   considering elemental hotspots for conservation is akin to calls for considering species

583   interactions (Tylianakis *et al.* 2010; Harvey *et al.* 2017) – i.e., levels of biodiversity beyond the

584   species that may be critical to maintain ecosystem functioning. We provide an analytical pipeline

585   to begin identifying elemental hotspots across landscapes. Equally, however, we provide an

586   analytical pipeline with the potential to identify areas to protect. For example, our analyses

587   suggest several areas that stand out as hot/coldspots of elemental dissimilarity (e.g., the yellow

588   patches present at grain size 500 m in Fig. 4). If future research demonstrates that these patterns

589   in elemental dissimilarity are reflected in species diversity as we have hypothesized, then our

590   analytical approach provides a tool to identify the specific areas (including area boundaries) to

591   protect.

592

593   Geological processes and abiotic factors have historically been the point of focus for predicting

594   elemental concentrations at local study sites, but recent works have shed light on the significance

595   of biotic ecosystem components on elemental distribution (Gounand *et al.* 2018; Schmitz *et al.*

596   2018; McInturf *et al.* 2019; Schmitz & Leroux 2020; Malhi *et al.* 2022). Biotic and abiotic

597   processes affecting the distribution of elements are often interdependent. By integrating both

598   perspectives, meta-ecosystem theory illustrates the intimate feedback between the biotic and

599   abiotic components of ecosystems, and how patch-specific biotic (e.g., organismal dispersal) and

600   abiotic (e.g., inorganic nutrient runoff) processes can lead to the emergence of regional scale

601   phenomena (Loreau *et al.* 2003; Massol *et al.* 2011, 2017). However, beyond theoretical and

602   conceptual advancements, we are still missing a coherent empirical framework to i) study and

603   analyse empirical patterns of elemental distribution in space and across spatial grains, and ii) to

604   link those abiotic observations (including information on longer timescale abiotic drivers such as

605   weathering of parent geological material) to the biotic component of ecosystems. We are

606   optimistic that our community perspective on elemental resources helps develop an empirical

607   framework initially to enhance our descriptions of ecosystems and understanding of how

608   elemental distributions scale with spatial gradients across different ecosystem types (see Table

609   1). We feel that our work provides the foundation upon which future work can attempt to address

610   (ii) - linking the abiotic observations to the biotic components, thus truly bridging these distinct

611   ecosystem compartments.

612

613   **Acknowledgements**

617
618

References

Ågren, G.I. & Weih, M. (2012). Plant stoichiometry at different scales: element concentration

   patterns reflect environment more than genotype. *New Phytol.*, 194, 944–952.

Anderson, M.J., Crist, T.O., Chase, J.M., Vellend, M., Inouye, B.D., Freestone, A.L., *et al.*

   (2011). Navigating the multiple meanings of β diversity: a roadmap for the practicing

   ecologist. *Ecol. Lett.*, 14, 19–28.

Balluffi-Fry, J., Leroux, S.J., Wiersma, Y.F., Heckford, T.R., Rizzuto, M., Richmond, I.C., *et al.*

   (2020). Quantity–quality trade-offs revealed using a multiscale test of herbivore resource

   selection on elemental landscapes. *Ecol. Evol.*, 10, 13847–13859.

Barton, P.S., Cunningham, S.A., Manning, A.D., Gibb, H., Lindenmayer, D.B. & Didham, R.K.

   (2013). The spatial scaling of beta diversity. *Glob. Ecol. Biogeogr.*, 22, 639–647.

Bernhardt, E.S., Blaszczak, J.R., Ficken, C.D., Fork, M.L., Kaiser, K.E. & Seybold, E.C. (2017).

   Control points in ecosystems: moving beyond the hot spot hot moment concept.

   Ecosystems, 20, 665–682.

Bump, J.K., Bergman, B.G., Schrank, A.J., Marcarelli, A.M., Kane, E.S., Risch, A.C., *et al.*

   (2017). Nutrient release from moose bioturbation in aquatic ecosystems. *Oikos*, 126,

   389–397.

Chase, J.M. & Leibold, M.A. (2009). *Ecological niches: linking classical and contemporary*

   approaches. University of Chicago Press.

Collins, S.M., Oliver, S.K., Lapierre, J., Stanley, E.H., Jones, J.R., Wagner, T., *et al.* (2017).

   Lake nutrient stoichiometry is less predictable than nutrient concentrations at regional

   and sub-continental scales. *Ecol. Appl.*, 27, 1529–1540.

Díaz, S.M., Settele, J., Brondízio, E., Ngo, H., Guèze, M., Agard, J., *et al.* (2019). The global

   assessment report on biodiversity and ecosystem services: Summary for policy makers.

643   Dodds, D.G. (1960). Food competition and range relationships of moose and snowshoe hare in

644   Newfoundland. *J. Wildl. Manag.*, 24, 52–60.

645   Doherty, T.S. & Driscoll, D.A. (2018). Coupling movement and landscape ecology for animal

646   conservation in production landscapes. *Proc. R. Soc. B Biol. Sci.*, 285, 20172272.

647   Edwards, R. (1998). The hyporheic zone. In: *River Ecology and Management*. Springer-Verlag,

648   New York, pp. 399–429.

649   Ellis-Soto, D., Ferraro, K.M., Rizzuto, M., Briggs, E., Monk, J.D. & Schmitz, O.J. (2021). A

650   methodological roadmap to quantify animal-vectored spatial ecosystem subsidies. *J.*

651   *Anim. Ecol.*, 90, 1605–1622.

652   Elser, J.J., Dobberfuhl, D.R., MacKay, N.A. & Schampel, J.H. (1996). Organism Size, Life

653   History, and N:P Stoichiometry. *BioScience*, 46, 674–684.

654   Frazier, A.E. (2022). Scope and its role in advancing a science of scaling in landscape ecology.

655   *Landsc. Ecol.*, 1–7.

656   Galbraith, E.D. & Martiny, A.C. (2015). A simple nutrient-dependence mechanism for predicting

657   the stoichiometry of marine ecosystems. *Proc. Natl. Acad. Sci.*, 112, 8199–8204.

658   Gharajehdaghipour, T., Roth, J.D., Fafard, P.M. & Markham, J.H. (2016). Arctic foxes as

659   ecosystem engineers: increased soil nutrients lead to increased plant productivity on fox

660   dens. *Sci. Rep.*, 6, 1–7.

661   Gounand, I., Harvey, E., Little, C.J. & Altermatt, F. (2018). Meta-ecosystems 2.0: rooting the

662   theory into the field. *Trends Ecol. Evol.*, 33, 36–46.

663   Hall, S.R. (2009). Stoichiometrically explicit food webs: feedbacks between resource supply,

664   elemental constraints, and species diversity. *Annu. Rev. Ecol. Evol. Syst.*, 40, 503.

665   Hall, S.R., Leibold, M.A., Lytle, D.A. & Smith, V.H. (2004). Stoichiometry and planktonic

666   grazer composition over gradients of light, nutrients, and predation risk. *Ecology*, 85,

667   2291–2301.

668   Harpole, W.S., Ngai, J.T., Cleland, E.E., Seabloom, E.W., Borer, E.T., Bracken, M.E., *et al.*

669   (2011). Nutrient co-limitation of primary producer communities. *Ecol. Lett.*, 14, 852–

670   862.

671   Harrison, S., Ross, S.J. & Lawton, J.H. (1992). Beta diversity on geographic gradients in Britain.

672   *J. Anim. Ecol.*, 151–158.

673   Harvey, E., Gounand, I., Ward, C.L. & Altermatt, F. (2017). Bridging ecology and conservation:

674   from ecological networks to ecosystem function. *J. Appl. Ecol.*, 54, 371–379.

675   Heckford, T.R., Leroux, S.J., Vander Wal, E., Rizzuto, M., Balluffi-Fry, J., Richmond, I.C., *et al.*

676   (2022). Spatially explicit correlates of plant functional traits inform landscape patterns of

677   resource quality. *Landsc. Ecol.*, 37, 59–80.

678   Helfield, J.M. & Naiman, R.J. (2001). Effects of salmon-derived nitrogen on riparian forest

679   growth and implications for stream productivity. *Ecology*, 82, 2403–2409.

680   Hundertmark, K.J. (1998). Home range, dispersal and migration. *Ecol. Manag. North Am. Moose*

681   *Smithson. Inst. Press Wash. DC USA*, 303–335.

682   Jeyasingh, P.D., Cothran, R.D. & Tobler, M. (2014). Testing the ecological consequences of

683   evolutionary change using elements. *Ecol. Evol.*, 4, 528–538.

684   Kaspari, M. (2020). The seventh macronutrient: how sodium shortfall ramifies through

685   populations, food webs and ecosystems. *Ecol. Lett.*, 23, 1153–1168.

686   Kaspari, M., Chang, C. & Weaver, J. (2010). Salted roads and sodium limitation in a northern

687   forest ant community. *Ecol. Entomol.*, 35, 543–548.

688   Kaspari, M. & Powers, J.S. (2016). Biogeochemistry and Geographical Ecology: Embracing All

689   Twenty-Five Elements Required to Build Organisms. *Am. Nat.*, 188, S62–S73.

690   Knecht, M.F. & Göransson, A. (2004). Terrestrial plants require nutrients in similar proportions.

691   *Tree Physiol.*, 24, 447–460.

692   Koleff, P. & Gaston, K.J. (2002). The relationships between local and regional species richness

693   and spatial turnover. *Glob. Ecol. Biogeogr.*, 11, 363–375.

694   Laliberté, E., Schweiger, A.K. & Legendre, P. (2020). Partitioning plant spectral diversity into

695   alpha and beta components. *Ecol. Lett.*, 23, 370–380.

696   Legendre, P. & De Cáceres, M. (2013). Beta diversity as the variance of community data:

697   dissimilarity coefficients and partitioning. *Ecol. Lett.*, 16, 951–963.

698   Legendre, P. & Gallagher, E.D. (2001). Ecologically meaningful transformations for ordination

699   of species data. *Oecologia*, 129, 271–280.

700   Leimgruber, P., McShea, W.J., Brookes, C.J., Bolor-Erdene, L., Wemmer, C. & Larson, C.

701   (2001). Spatial patterns in relative primary productivity and gazelle migration in the

702   Eastern Steppes of Mongolia. *Biol. Conserv.*, 102, 205–212.

703   Leroux, S.J. & Schmitz, O.J. (2015). Predator-driven elemental cycling: The impact of predation

704   and risk effects on ecosystem stoichiometry. *Ecol. Evol.*, 5, 4976–4988.

705   Leroux, S.J., Wal, E.V., Wiersma, Y.F., Charron, L., Ebel, J.D., Ellis, N.M., *et al.* (2017).

706   Stoichiometric distribution models: ecological stoichiometry at the landscape extent.

707   *Ecol. Lett.*, 20, 1495–1506.

708   Loreau, M., Daufresne, T., Gonzalez, A., Gravel, D., Guichard, F., Leroux, S.J., *et al.* (2013).

709   Unifying sources and sinks in ecology and E arth sciences. *Biol. Rev.*, 88, 365–379.

710   Loreau, M., Mouquet, N. & Holt, R.D. (2003). Meta-ecosystems: a theoretical framework for a

711   spatial ecosystem ecology. *Ecol. Lett.*, 6, 673–679.

712   Maathuis, F.J. (2009). Physiological functions of mineral macronutrients. *Curr. Opin. Plant*

713   *Biol.*, 12, 250–258.

714   Malhi, Y., Lander, T., le Roux, E., Stevens, N., Macias-Fauria, M., Wedding, L., *et al.* (2022).

715   The role of large wild animals in climate change mitigation and adaptation. *Curr. Biol.*,

716   32, R181–R196.

717   Marleau, J.N., Guichard, F. & Loreau, M. (2015). Emergence of nutrient co-limitation through

718   movement in stoichiometric meta-ecosystems. *Ecol. Lett.*, 18, 1163–1173.

719   Marrs, R.H., Lee, H., Blackbird, S., Connor, L., Girdwood, S.E., O'Connor, M., *et al.* (2020).

720   Release from sheep-grazing appears to put some heart back into upland vegetation: A

721   comparison of nutritional properties of plant species in long-term grazing experiments.

722   *Ann. Appl. Biol.*, 177, 152–162.

723   Massol, F., Altermatt, F., Gounand, I., Gravel, D., Leibold, M.A. & Mouquet, N. (2017). How

724   life-history traits affect ecosystem properties: effects of dispersal in meta-ecosystems.

725   *Oikos*, 126, 532–546.

726   Massol, F., Gravel, D., Mouquet, N., Cadotte, M.W., Fukami, T. & Leibold, M.A. (2011).

727   Linking community and ecosystem dynamics through spatial ecology. *Ecol. Lett.*, 14,

728   313–323.

729   Mayor, S.J., Schaefer, J.A., Schneider, D.C. & Mahoney, S.P. (2009). The spatial structure of

730   habitat selection: a caribou's-eye-view. *Acta Oecologica*, 35, 253–260.

731   McCann, K.S., Hastings, A. & Strong, D.R. (1998). Trophic cascades and trophic trickles in

732   pelagic food webs. *Proc. R. Soc. Lond. B Biol. Sci.*, 265, 205–209.

733 McClain, M.E., Boyer, E.W., Dent, C.L., Gergel, S.E., Grimm, N.B., Groffman, P.M., *et al.*

734   (2003). Biogeochemical Hot Spots and Hot Moments at the Interface of Terrestrial and

735   Aquatic Ecosystems. *Ecosystems*, 6, 301–312.

736 McInturf, A.G., Pollack, L., Yang, L.H. & Spiegel, O. (2019). Vectors with autonomy: what

737   distinguishes animal-mediated nutrient transport from abiotic vectors? *Biol. Rev.*, 94,

738   1761–1773.

739 McIntyre, P.B., Flecker, A.S., Vanni, M.J., Hood, J.M., Taylor, B.W. & Thomas, S.A. (2008).

740   Fish distributions and nutrient cycling in streams: can fish create biogeochemical

741   hotspots. *Ecology*, 89, 2335–2346.

742 McNaughton, S., Ruess, R. & Seagle, S. (1988). Large mammals and process dynamics in

743   African ecosystems. *BioScience*, 38, 794–800.

744 Nakajima, N., Morikawa, H., Igarashi, S. & Senda, M. (1981). Differential effect of calcium and

745   magnesium on mechanical properties of pea stem cell walls. *Plant Cell Physiol.*, 22,

746   1305–1315.

747 Olesinski, J., Lavigne, M.B. & Krasowski, M.J. (2011). Effects of soil moisture manipulations

748   on fine root dynamics in a mature balsam fir (Abies balsamea L. Mill.) forest. *Tree*

749   *Physiol.*, 31, 339–348.

750 Parent, S.-É., Parent, L.E., Egozcue, J.J., Rozane, D.-E., Hernandes, A., Lapointe, L., *et al.*

751   (2013). The plant ionome revisited by the nutrient balance concept. *Front. Plant Sci.*, 4,

752   39.

753 Pastor, J., Dewey, B., Moen, R., Mladenoff, D.J., White, M. & Cohen, Y. (1998). Spatial

754   patterns in the moose–forest–soil ecosystem on Isle Royale, Michigan, USA. *Ecol. Appl.*,

755   8, 411–424.

756 Patrick, C.J. & Yuan, L.L. (2019). The challenges that spatial context present for synthesizing

757   community ecology across scales. *Oikos*, 128, 297–308.

758 Pichon, B., Thebault, E., Lacroix, G. & Gounand, I. (2023). Quality matters: stoichiometry of

759   resources modulates spatial feedbacks in aquatic-terrestrial meta-ecosystems. *bioRxiv*,

760   2023–03.

761 Poisot, T., Guéveneux-Julien, C., Fortin, M., Gravel, D. & Legendre, P. (2017). Hosts, parasites

762   and their interactions respond to different climatic variables. *Glob. Ecol. Biogeogr.*, 26,

763   942–951.

764 Pörtner, H.-O., Roberts, D.C., Adams, H., Adler, C., Aldunce, P., Ali, E., *et al.* (2022). Climate

765   change 2022: Impacts, adaptation and vulnerability. *IPCC Sixth Assess. Rep.*

766 Reich, P.B., Oleksyn, J., Modrzynski, J., Mrozinski, P., Hobbie, S.E., Eissenstat, D.M., *et al.*

767   (2005). Linking litter calcium, earthworms and soil properties: a common garden test

768   with 14 tree species. *Ecol. Lett.*, 8, 811–818.

769 Rizzuto, M., Leroux, S.J., Vander Wal, E., Richmond, I.C., Heckford, T.R., Balluffi-Fry, J., *et al.*

770   (2021). Forage stoichiometry predicts the home range size of a small terrestrial herbivore.

771   *Oecologia*, 197, 327–338.

772 Rooney, N., McCann, K., Gellner, G. & Moore, J.C. (2006). Structural asymmetry and the

773   stability of diverse food webs. *Nature*, 442, 265.

774 Rooney, N., McCann, K.S. & Moore, J.C. (2008). A landscape theory for food web architecture.

775   *Ecol. Lett.*, 11, 867–881.

776 Schmitz, O.J. & Leroux, S.J. (2020). Food webs and ecosystems: linking species interactions to

777   the carbon cycle. *Annu. Rev. Ecol. Evol. Syst.*, 51, 271–295.

778   Schmitz, O.J., Wilmers, C.C., Leroux, S.J., Doughty, C.E., Atwood, T.B., Galetti, M., *et al.*

779   (2018). Animals and the zoogeochemistry of the carbon cycle. *Science*, 362, eaar3213.

780   Sentis, A., Haegeman, B. & Montoya, J.M. (2022). Stoichiometric constraints modulate

781   temperature and nutrient effects on biomass distribution and community stability. *Oikos*,

782   2022.

783   Shurin, J.B., Gruner, D.S. & Hillebrand, H. (2006). All wet or dried up? Real differences

784   between aquatic and terrestrial food webs. *Proc. R. Soc. B Biol. Sci.*, 273, 1–9.

785   Sterner, R.W. & Elser, J.J. (2017). Ecological stoichiometry. In: *Ecological Stoichiometry*.

786   Princeton University Press.

787   Tucker, M.A., Böhning-Gaese, K., Fagan, W.F., Fryxell, J.M., Van Moorter, B., Alberts, S.C., *et*

788   *al.* (2018). Moving in the Anthropocene: Global reductions in terrestrial mammalian

789   movements. *Science*, 359, 466–469.

790   Tylianakis, J.M., Laliberté, E., Nielsen, A. & Bascompte, J. (2010). Conservation of species

791   interaction networks. *Biol. Conserv.*, 143, 2270–2279.

792   Wang, X., Blanchet, F.G. & Koper, N. (2014). Measuring habitat fragmentation: An evaluation

793   of landscape pattern metrics. *Methods Ecol. Evol.*, 5, 634–646.

794   Ward, C.L., McCann, K.S. & Rooney, N. (2015). HSS revisited: multi-channel processes

795   mediate trophic control across a productivity gradient. *Ecol. Lett.*, 18, 1190–1197.

796   Whittaker, R.H. (1972). Evolution and measurement of species diversity. *Taxon*, 213–251.

797   Wilkinson, S.R., Grunes, D.L. & Sumner, M.E. (2000). Nutrient interactions in soil and plant

798   nutrition. In: *Handbook of Soil Science*. CRC Press, Boca Raton, Fl.

799   Wu, J., Naeem, S., Elser, J., Bai, Y., Huang, J., Kang, L., *et al.* (2015). Testing biodiversity-

800   ecosystem functioning relationship in the world's largest grassland: overview of the

801   IMGRE project. *Landsc. Ecol.*, 30, 1723–1736.

802   Zhang, S., Zhang, J., Slik, J.F. & Cao, K. (2012). Leaf element concentrations of terrestrial

803   plants across China are influenced by taxonomy and the environment. *Glob. Ecol.*

804   *Biogeogr.*, 21, 809–818.

805

806

807 **Tables**

808 **Table 1.** Testable hypotheses generated from our proof of concept.

Metric	Hypothesis	Example of data
Elemental Dissimilarity	Spatial grain at which the change in elemental dissimilarity is the greatest is also the grain size at which organisms are most active in their foraging	Elemental data of forage species Telemetry data for consumer species
	Dissimilarity in resource elements follow general patterns with spatial scale	Elemental data of soil Elemental data of individual forage species
	Changes in dissimilarity of elements with spatial scale should be reflected in the structure of biotic communities. Specifically: 1. Low spatial turnover in resource elements should lead to the assembly of functionally more similar species, a lower alpha-diversity, and a generally lower functioning level (i.e. saturation is	Elemental data of soil Species diversity data

reached faster because of functional

redundancy amongst species).

2. High spatial turnover in elements,

    on the other hand, should lead to

    more functional complementarity

    and generally higher functioning

    level. In particular, lower local

    evenness of elements should lead to

    dominance by a few species that

    are able to maximize their use of

    most elements being at very low

    level (R*).

Local contribution to elemental dissimilarity	Localized hot and cold spots of elemental dissimilarity should reflect localized hot and cold spots of species diversity at finer grain sizes and hot and cold spots of landscape diversity (i.e. aquatic-terrestrial boundaries) at large grain sizes	Diversity surveys Satellite imagery
	Alternatively, local hot and cold spots of elemental dissimilarity could emerge through the movement of organisms across the landscape	Telemetry Theoretical models

| Elemental contribution to dissimilarity | Elements may differentially indicate areas of high biodiversity - for example tree species with calcium-rich detritus support greater diversity and biomass of earthworms (Reich et al. 2005). | Biodiversity surveys in areas where calcium is the most important element contributing to elemental diversity |
| | Alternatively, selective herbivory for limiting nutrients could lead to elemental cold spots | Herbivory surveys in areas where calcium is depleted |

809

810

811   **Figures**

Building StDM from white birch foliage using 6 landscape covariates

Data Processing Steps

3 sets (n = 3) of 6 subsamples
(ss = 6) at grain size (s)

A Community Ecology of Elements

812

40

(a)
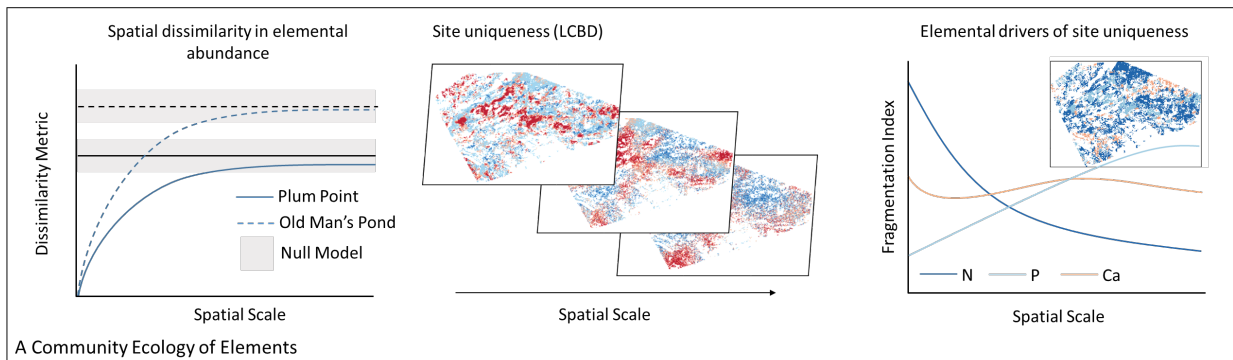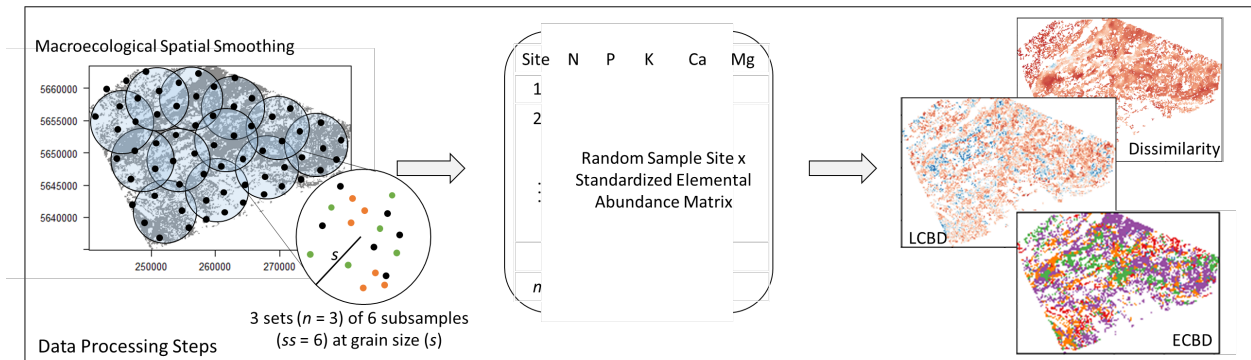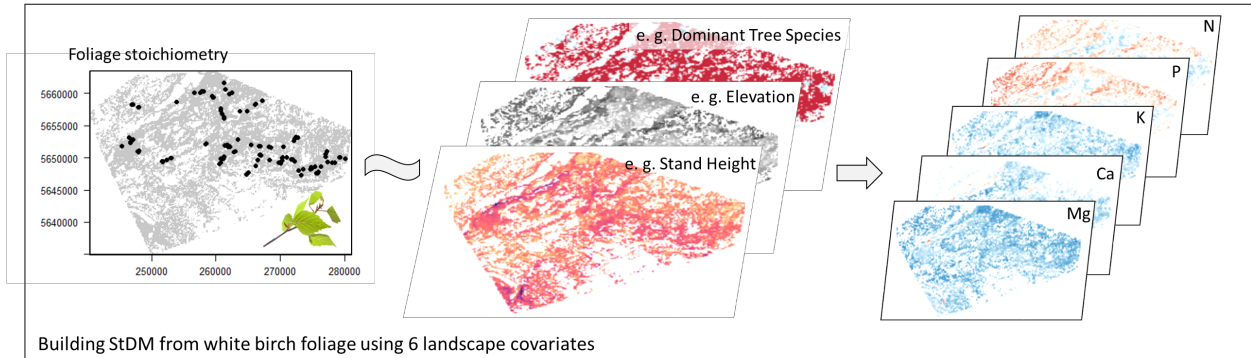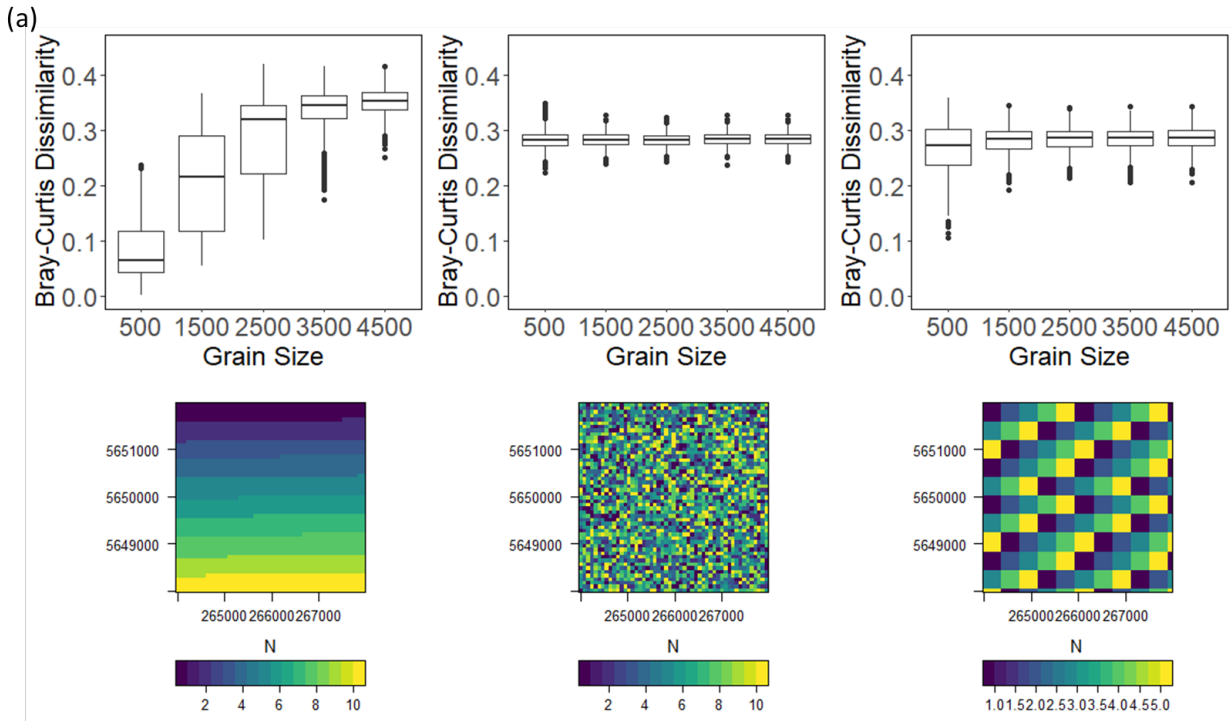
(b)

	Patchy Landscape		Random Landscape		Checkerboard Landscape	
	N	Mg	N	Mg	N	Mg
Mean Core Area	0	0	0.01	0.02	5.08	5.32
Perimeter Area Fractal Dimension	1.75	1.93	1.70	1.73	1.03	1.14
Normalized Landscape Shape Index	0.54	0.54	0.74	0.75	0.19	0.18

813

41
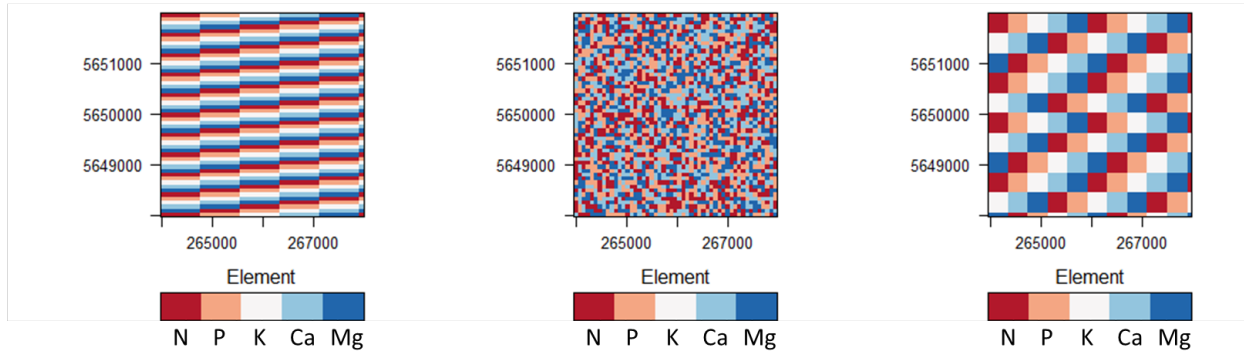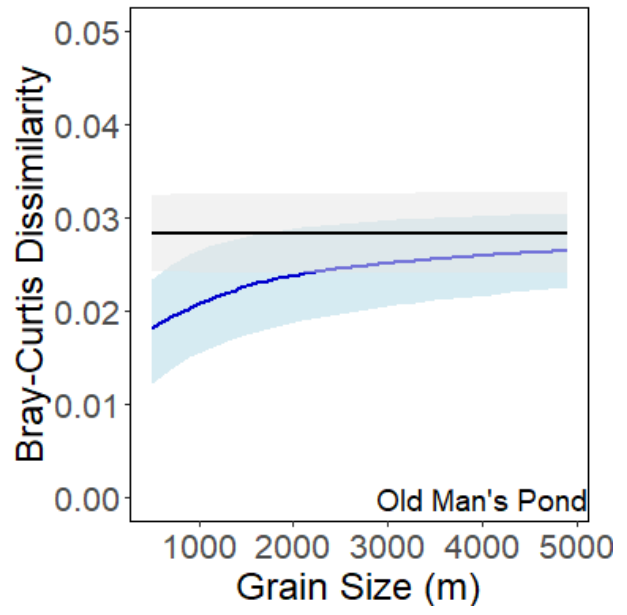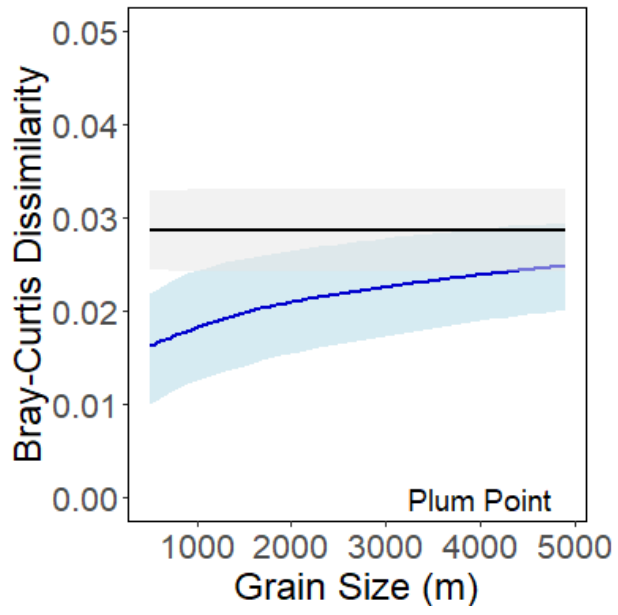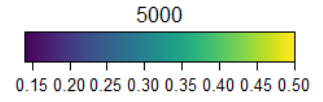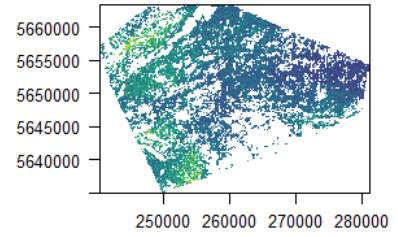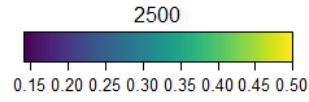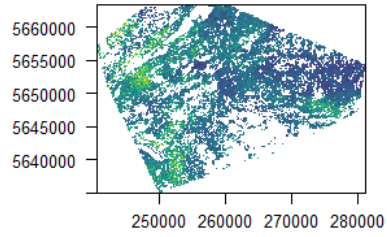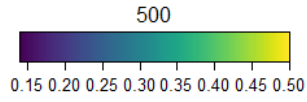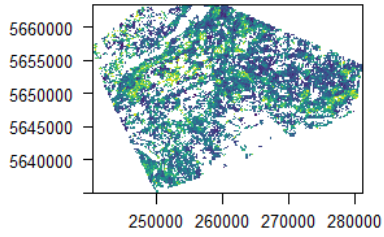
817
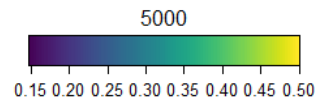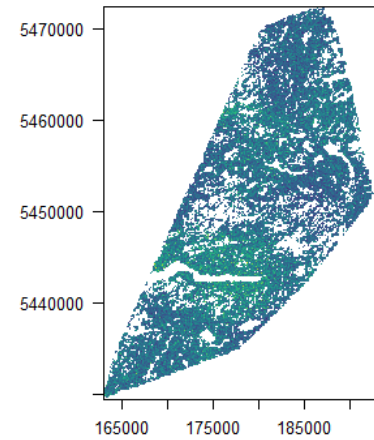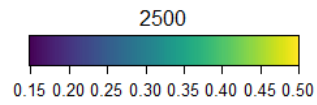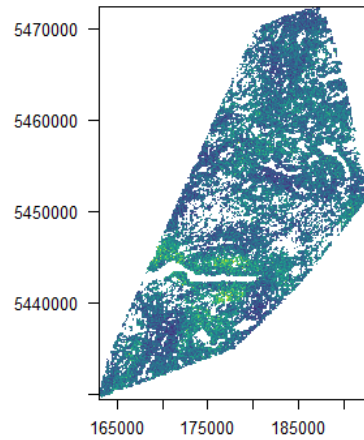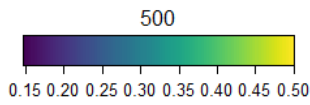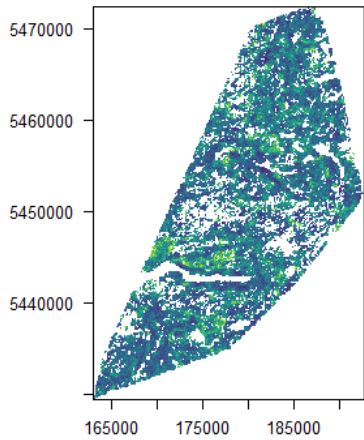
818

819

820
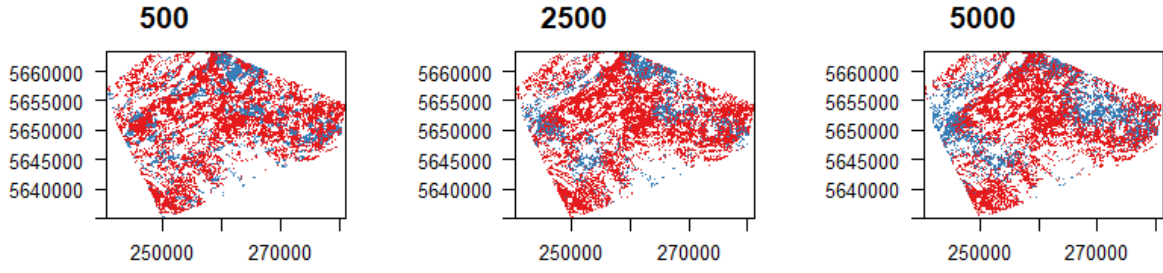
821
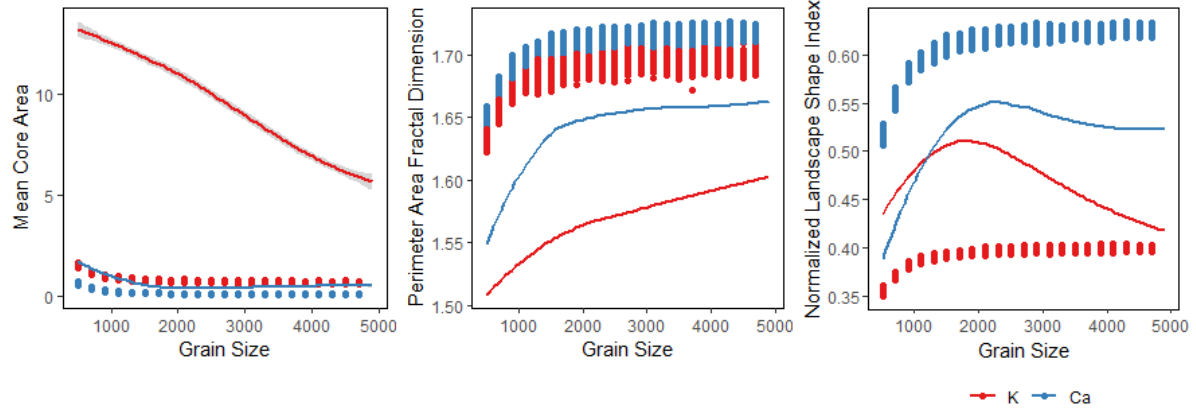
822

823   (a)
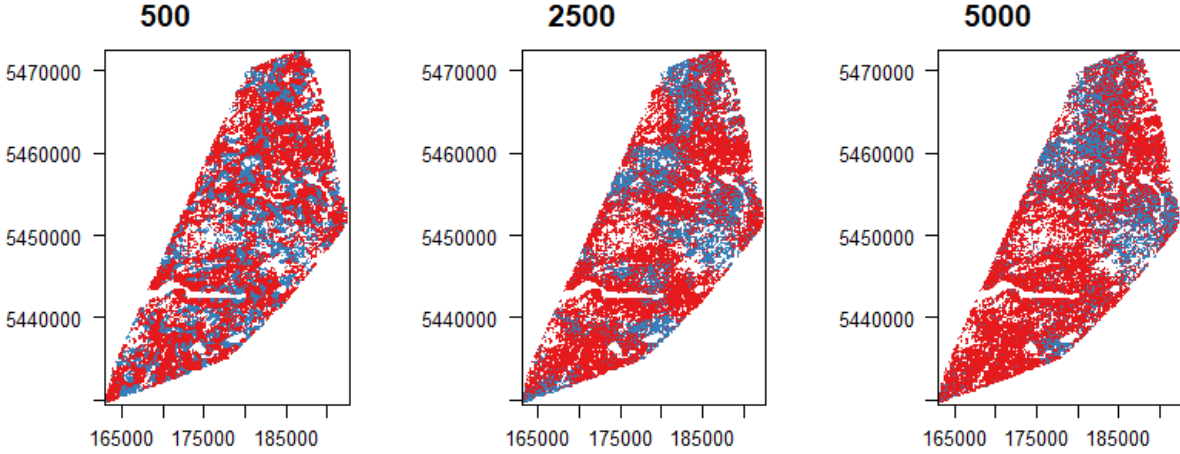

824
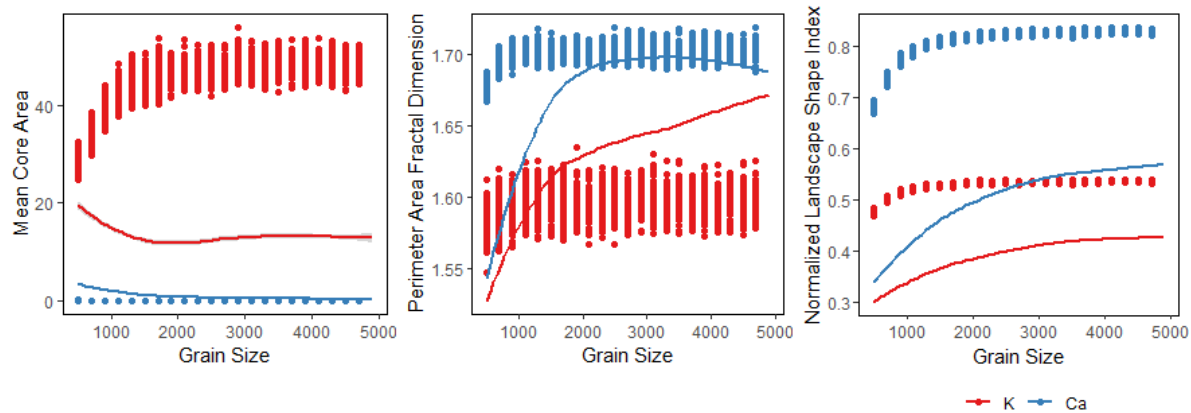
825

826   (b)

827

828   **Figure Captions**

829   **Figure 1.** The empirical framework can be outlined in three steps. First, we build a

830   stoichiometric distribution model (sensu Leroux et al. 2017) for each of our five key elements

831   from white birch foliage using three landscape covariates (normalized aspect, slope, and

832   elevation) and three categorical landscape covariates (landcover, stand height, and dominant tree

833   species) to predict stoichiometric composition for foliage in each cell. Then, we apply the macro-

834   ecological spatial smoothing approach proposed by Patrick and Yuan (2019) to resample and

835   summarize local observations at increasingly large grain sizes to determine how community

836   metrics (dissimilarity, local contribution to dissimilarity, and elemental contribution to

837   dissimilarity) applied to elemental composition varied with spatial scale. We apply this approach

838   to both the landscapes and a randomization, null model, of each landscape. Finally, we report

839   how our three community metrics - dissimilarity in elemental composition, local contribution to

840   dissimilarity, and elemental contribution to dissimilarity – vary with spatial scale.

841   **Figure 2.** Demonstration of how (a) dissimilarity changes with grain sizes for different

842   hypothetical landscapes – one in which elemental composition exists in a predictable gradient,

843   another randomized landscape, and a third where elemental composition is a checkerboard of

844   high composition and low composition. Demonstration of how (b) patch metrics change with

845   different hypothetical patch configurations – one where patches are organized rectilinearly on the

846   landscape, one where patches and randomly scattered across the landscape, and a third where the

847   patches are an even checkerboard. Recall patch class is based on which of the five elements has

848   been ranked most important contributor to pixel dissimilarity. In both (a) and (b) the numbers on

849   the x- and y- axes are in UTM coordinates.

850   **Figure 3.** Relationship between elemental dissimilarity indices and grain size for Plum Point and

851   Old Man's Pond. Here, the observed data is presented in blue with the mean value in dark blue

852   and the light blue indicating the standard deviation, while the black line indicates the mean value

853   of null model simulations (where the location of each site is randomly moved in the landscape)

854   with the light grey indicating the standard deviation.

855   **Figure 4.** LCBD across the two landscapes (Plum Point top, Old Man's Pond bottom) at three

856   different grain sizes where the x- and y-axes are in UTM coordinates. Here, blue indicate sites

857   that contribute more than average to beta-diversity, while red indicates sites that contribute less

858   than average to beta-diversity. Note that a site can contribute more than average to beta-diversity

859   by being either more nutrient-rich or nutrient-poor than the average site. See Fig. A1 in

860   Supplementary Information 1 for map of study area locations.

861   **Figure 5.** Landscape plotted by which element contributes the most to its beta diversity for three

862   representative grain sizes (500, 2500, and 5000 m) for (a) Plum Point and (b) Old Man's Pond

863   where red is K and blue is Ca and white cells are areas without forests (e.g., lakes, rivers, roads).

864   Bottom row in both a) and b) illustrates of how landscape metrics measuring how patches with

865   the same top elemental driver of beta diversity (ECBD) change with grain size for each element.

866   Here the lines indicate the observed data while the points are the results from the null model. See

867   Fig. A1 in Supplementary Information 1 for map of study area locations.

868